https://doi.org/10.1016/j.engstruct.2021.112394

Comparative Life Cycle Assessment of Composite Structures Incorporating Uncertainty and Global Sensitivity Analysis

Menghan Zhao, You Dong, and Hongyuan Guo

Abstract: In recent years, there have been increasing efforts seeking novel material and structural alternatives to alleviate environmental and economic burdens caused by conventional engineering structures. However, research on long-term environmental impact and cost of the design alternatives are limited. This paper presents a comparative life-cycle assessment (LCA) and life-cycle cost analysis (LCCA) of three composite columns over a service life of 100 years. The studied cases are typical composite structural forms consisting of: (1) concrete-filled steel tubular column (CFST); (2) concrete-filled fiber-reinforced polymer (FRP) tubular column (CFFT); and (3) hybrid FRP-concrete-steel double-skin tubular column (DSTC). The CFFT is expected to have extended service life due to corrosion resistance of FRP. The DSTC is designed to reduce concrete consumption by leaving a void at the center of the column. Both deterministic and probabilistic results are discussed in this research. Specifically, Sobol's index is selected to aid the probabilistic LCA and LCCA analyses. The deterministic LCA results indicate that CFFT has the least CO_2 emission: 50 % less than DSTC and 60 % less than CFST. While LCCA results show that for the investigated scenario the DSTC costs the most across the studied service life, about 15 % more than CFST and CFFT. The probabilistic results indicated that the production and maintenance stage are two significant influential factors of the LCA and LCCA results. In general, CFFT and DSTC are more economic and environmental-friendly alternatives compared to CFST.

Keywords: Fiber-reinforced polymer (FRP), concrete, steel, CO_2 emissions, life-cycle cost, uncertainty analysis.

1. Introduction

As concerns about environmental issues are raising constantly, construction environmental impact, one of the major sources of greenhouse gas emissions, has drawn more public attention. Infrastructure construction has been assessed to be responsible for one third of the global anthropogenic greenhouse gas (GHG) emissions and approximately the same share of the global energy production [1]. As two widely used construction materials, concrete and steel contribute massive portion of global CO_2 emission. In 2012 alone, the production of cement was approximately 3.8 giga tonnes (Gt), approximately equal to 3.2 Gt of CO_2 emissions worldwide, around 8 % of the annual anthropogenic CO_2 emissions [2]. The carbon intensity of steel production varies among manufacturing techniques, data has shown that the average CO_2 emission is 1.9 t CO_2 per tonne of steel production [3].

To mitigate these environmental impacts triggered by concrete and steel production, industries have attempted to substitute conventional materials with alternatives, such as recycled concrete [4-7], ultra-high performance concrete (UHPC) [8, 9], stainless steel [10], etc., which have been proved to show better performance from a life-cycle perspective [11-13]. Apart from innovation at the material level, another concept of integrating multiple novel materials into structural elements (e.g., concrete-filled steel tubular and concrete-fill FRP tubular columns) has gained momentum. Concrete-filled steel tubular columns (CFSTs) offer a variety of structural benefits including high strength, superior fire resistance, outstanding ductility, and great energy absorption capacity [14]. In addition, with the outer steel tube acting as shuttering, the construction cost and duration could be reduced accordingly. Nevertheless, corrosion issue must be considered under marine circumstances, where FRP-concrete composite structures may become a better option for its corrosion-resistance characteristic. Likewise, the FRP confinements can also be used as permanent shuttering of concrete. The applied FRP jackets can be fabricated by pultrusion, wet lay-up or filament winding techniques, and are light-weighted enough to be easily shipped from plants to construction sites [15]. Wet lay-up (e.g., FRP wraps) is more commonly used in retrofitting existing structures while pultrusion (e.g., FRP bars) and filament winding (e.g., prefabricated FRP tubes) are more suitable for constructing new constructions. Filament-wound FRP tubes are widely used in fabricating columns with plain or steel-reinforced concrete infilled, which are known as concrete-filled FRP tubular columns (CFFTs). CFFTs have been widely applied in new constructions such as bridge columns and piles due to the outstanding corrosion resistance [16-19]. Nevertheless, the major drawbacks to CFFTs are high initial costs, linear-elastic-brittle stress-strain behavior, low elastic modulus-to-strength ratio and inferior fire resistance [20]. To offset these disadvantages, an innovative structural form was proposed in [20], namely hybrid FRP-concrete-steel double-skin tubular columns (DSTCs). A DSTC consists of an inner steel tube and an outer FRP tube with concrete filled in between, which is expected to be more ductile and thus can be used in flexural and seismic conditions. It particularly benefits the need for sustainable construction as the presence of the inner void largely reduces concrete without significant strength loss. Furthermore, DSTC holds great potential for associating with high-strength concrete [21, 22] and even UHPC [23-25].

While CFSTs, CFFTs, and DSTCs have been extensively studied regarding their mechanical properties and structural performance [14, 26-31], limited efforts have been devoted to investigating life-cycle performance of such hybrid structures and more studies should be conducted on relevant research area. Steel, steel-concrete composite column with steel reinforcement and wooden column were investigated from a life-cycle perspective while the scope only covered the cradle-to-gate span without considering the end-of-life scenario [32]. Han [33, 34] did some studies on CFST regarding its structural deterioration throughout the lifespan, the results, however, were neither economy nor environment-oriented. A nonmonetary evaluation model was developed to identify the life-cycle benefit-cost of CFST and FRP-confined concrete structures [35], which was further refined to an advanced framework that utilizes material properties to assess the performance-based life-cycle cost of composite materials in construction [36]. Other studies were carried out to compute life-cycle cost or environmental impacts of FRP reinforced concrete, FRP components or structures [37-43].

Life-cycle assessment (LCA) and life-cycle cost analysis (LCCA) are important techniques in the abovementioned studies, which have been widely used in buildings [44-46] and infrastructures [47-49]. LCA is a framework developed for evaluating life-cycle environmental performance of a product system, including raw material acquisition, production, construction, use, disposal, and transportation required during the process [50]. While LCCA is a supplementary method to LCA, which employs life-cycle principles to account for all costs incurred over a system's lifetime rather than just initial cost [51]. The analysis has to be completed by aggregating all life-cycle inventories (LCI) associated with every unit process. Dozens of LCI models have been developed, which can be classified into evaluation at midpoint (e.g. CML 2002, EDIP 97-2003, MEEuP and TRACI), endpoint (e.g. Eco-indicator 99 and EPS 2000), or combined (e.g. Impact 2002, Swiss Ecoscarcity 06, ReCiPe 2008) [52]. Midpoint impact categories include global warming potential (GWP), primary energy (PE), acidification potential, eutrophication potential, human toxicity potential, ozone layer depletion potential, and photochemical smog formation potential. While endpoint focuses more on receptors including resources (R), ecosystem quality (EQ), climate change (CC) and human health (HH) [53]. GWP, one of the most concerned midpoint categories [53], is selected in this study. In the context of infrastructure, life-cycle cost comprises agency cost, user cost, and environmental cost, except that environmental cost is rarely considered [54]. As this research focuses on LCCA of structural component rather than system, only agency cost is evaluated herein.

Most of the previous research regarding composite structures are presented in a deterministic manner without considering uncertainties embedded in the assessment process [55]. The outcome of the assessment model is affected by uncertainty (e.g. physical properties of materials, amount of pollutants emitted, etc.). Uncertainty plays a significant role within the life-cycle assessment process and the effect of various uncertainty on the life-cycle performance could be very different. It is of vital importance to take the uncertainties with the assessment process in a life-cycle context [56-59]. Without considering the uncertainty may introduce some arbitrariness in the comparison of different design options. A common practice to study the effect of uncertainties on output is performing sensitivity analyses. Most of the sensitivity analyses focused on the linearity by varying one parameter at a time, as such, the effect of the varied parameters can be reflected individually [41]. Another approach requires input as probabilistic parameters rather than centered values, by which the extent of each input parameter contributing to the output variance can be determined [42]. These two methods belong to the realm of local sensitivity analysis and global sensitivity analysis, respectively [55]. The global sensitivity analysis varies all the variables simultaneously and the random variable changes through its entire range. In this paper, Sobol's method is selected to perform global sensitivity analysis for its capability of determining the critical input parameter, i.e., parameter that contributes the most to the output variance and therefore should be most accurately known. Parameters with low Sobol indices can be removed, as their contribution to the overall variance is insignificant and thus have marginal effect on the output. Furthermore, Sobol's method is capable of identifying interaction effect between multiple input parameters [60]. It has been proved by many researchers that Sobol's method performed well on uncertainty treatment in LCA [55, 60-63]. To the best knowledge of the authors, there has been no studies focusing on the probabilistic performance assessment and global sensitivity analysis of CFST, CFFT, and DSTC in a life cycle context.

To address the current research gap, this paper aims to investigate deterministic and probabilistic life-cycle performance of CFST, CFFT, and DSTC from environmental and economic perspectives. Given three comparable composite structural cases, life-cycle assessment and life-cycle cost analysis (LCA-LCCA), an approach that leads to long-term and preventive assessment [54], is used in this study. The remainder of the paper is structured as follows: Section 2 elaborates the investigated structural forms including material and structural design, followed by a detailed introduction of the life-cycle model in Section 3. Section 4 presents the computational process of the deterministic life-cycle environmental impact and cost results while the accordingly probabilistic results are summarized in Section 5.

2. Investigated structural elements

To demonstrate benefits of the novel structural systems (i.e. CFFT and DSTC) over traditional CFST, fair comparison should be made among three. Herein, the case of traditional column CFST is directly taken from [32], in which the strength, stability and stiffness were all taken into account on the basis of Eurocode 3 [64] and Eurocode 4 [65]. [32] calculated the axial bearing capacity as follows: 1. Consider a slab in a three-story building with panel dimension of 10 × 20 m^2; 2. Take appropriate dead and live loads for the slab in accordance with the standards; and 3. Transform dead and live loads into uniaxial load on a column of 5,622 kN. Therefore, CFFT and DSTC are both designed to carry nominal axial load of 5,622 kN. Fig. 1 illustrates the loading condition and cross-section profiles of the investigated columns. CFST consists of an outer steel tube and steel reinforced concrete. CFFT comprises with a tubular FRP tube and a concrete core while DSTC includes an FRP tube, an inner steel tube and an annular concrete infill.

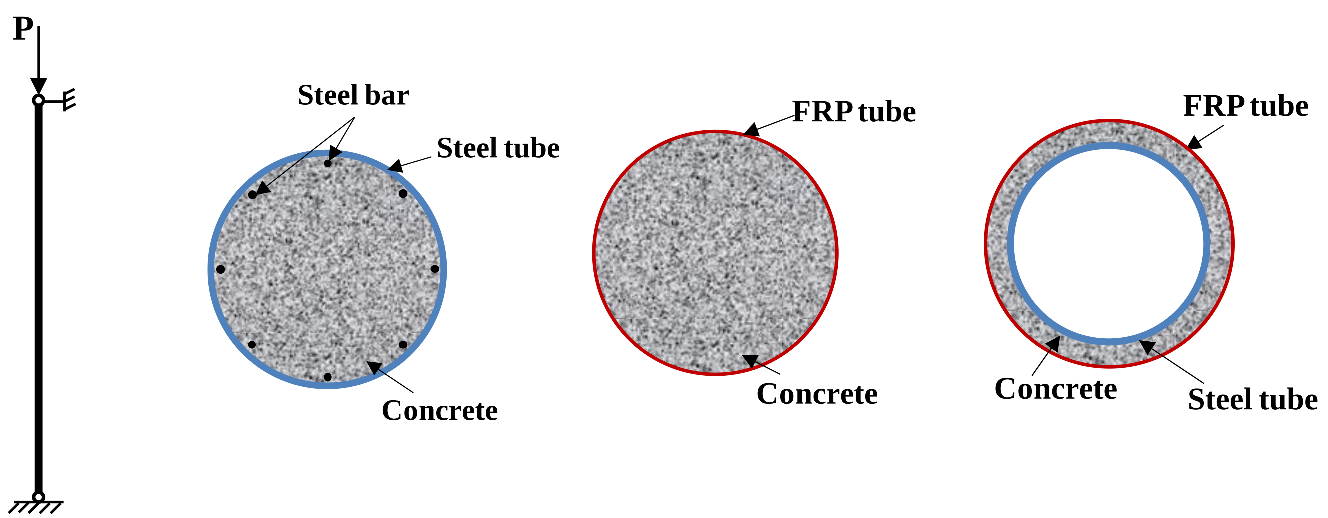

a. Loading condition b. CFST c. CFFT d. DSTC

Fig. 1. Column loading condition and cross-section profiles

2.1 Material design

Materials used for the three design alternatives are tabulated in Table 1. The benchmark example is an excerpt from [32], where 1 m^3 of concrete production considers 400 kg of cement, 700 kg of sand, and 1200 kg of gravel. While for the other two scenarios, 1 m^3 of C40 concrete requires 350 kg of cement, 175 kg of water, 1194 kg of sand, and 614 kg of gravel [66]. A typical density of 7850 kg/m^3 is assigned to steel. Filament-wound glass FRP is assumed to act as confinement for CFFT and DSTC. Material properties of GFRP and steel tube (for CFFT and DSTC) are taken from the experimental results in [22].

2.2 Structural design

To make a fair comparison, CFFT and DSTC are supposed to be designed to have similar loading capacity with CFST. To this end, the theoretical model proposed in [67] is used to determine geometric parameters of CFFT and DSTC. The model in [67] has been verified against extensive database [68-70]. This design method is described as follows:

Firstly, the confinement stiffness ratio ρ_κ and strain ratio ρ_ε are calculated as follows

$$\rho_\kappa = \frac{2E_{frp}t_{frp}}{\left(f'_{co}/\varepsilon_{co}\right)D} \tag{1}$$

$$\rho_\varepsilon = \frac{\varepsilon_{h,rup}}{\varepsilon_{co}} \tag{2}$$

where E_{frp} = elastic modulus of the FRP in the hoop direction, t_{frp} = thickness of the FRP tube, D = diameter of the confined concrete core, f'_{co} = unconfined concrete axial strength, ε_{co} = unconfined concrete axial strain, and $\varepsilon_{h,rup}$ = hoop rupture strain of FRP.

With the above two ratios determined, the ultimate axial strain ε_{cu} and the compressive strength f'_{cc} can be computed as

$$\frac{\varepsilon_{cu}}{\varepsilon_{co}} = 1.75 + 6.5\rho_\kappa^{0.8}\rho_\varepsilon^{1.45} \tag{3}$$

$$\text{Given } \rho_\kappa \geq 0.01, \frac{f'_{cc}}{f'_{co}} = 1 + 3.5\left(\rho_\kappa - 0.01\right)\rho_\varepsilon \tag{4}$$

It should be noted that for DSTC [71], the ultimate axial strain ε_{cu} becomes

$$\frac{\varepsilon_{cu}}{\varepsilon_{co}} = 1.75 + 6.5\rho_\kappa^{0.8}\rho_\varepsilon^{1.45}(1-\phi)^{-0.22} \tag{5}$$

where ϕ is void ratio, i.e., the ratio of outer diameter of the steel tube to diameter of the concrete core.

The abovementioned models [67, 71] have been proved to be able to accurately predict axial compressive strength of CFFT and DSTC via numerous experimental [72-75] and parametric studies [70, 76-78].

The loading capacity of CFFT equals the confined concrete strength multiplied by concrete area while that of DSTC approximately equals the load resisted by concrete and steel tube [73]. Given the loading capacity around 5,622 kN, iteration processes were conducted for CFFT [67] and DSTC [71] to determine the targeted cross-sectional parameters. The parameters so determined, together with those of CFST [32], are summarized in Table 1. The calculated loading capacity of CFFT and DSTC are 5,676 kN and 5,670 kN, respectively.

Table 1 Detailed information of the investigated elements

Component	Material property	CFST [32]	CFFT	DSTC
Steel tube	Yield strength f_y (MPa)	355	-	360
	Ultimate strength f_u (MPa)	-		491
	Outer diameter D_s (mm)	406		280
	Thickness t_s (mm)	6		8
Concrete	Compressive strength f'_{co} (MPa)	35	40	40
	Reinforcement area A_s (mm^2)	4517	-	-
GFRP tube	Elastic modulus E_{frp} (GPa)	-	44	44
	Inner diameter D (mm)	-	300	350
	Thickness t_{frp} (mm)	-	3.0	2.5

3. Life-cycle model

This section elucidates the studied life-cycle model. Material design of the illustrative examples is primarily described, which will be integrated with unit environmental and economic impact for final evaluation. The deterioration models for each alternative are then discussed, and in turn to define maintenance schemes [79]. To cover major maintenance actions for each alternative, FHWA [80] has suggested the investigated time period to be as long as enough. In balance, the life-cycle assessment herein is conducted over a period of 100 years. The results are also presented in a cumulative way for each year such that the results for any shorter period can be referenced.

Fig. 2 depicts the framework of life-cycle assessment consisting of goal and scope definition, inventory analysis, impact assessment, and interpretation of the results [50]. The following section will define the goal and scope of the LCA-LCCA, while the inventory analysis and impact assessment will be discussed in Section 4 along with the analysis results.

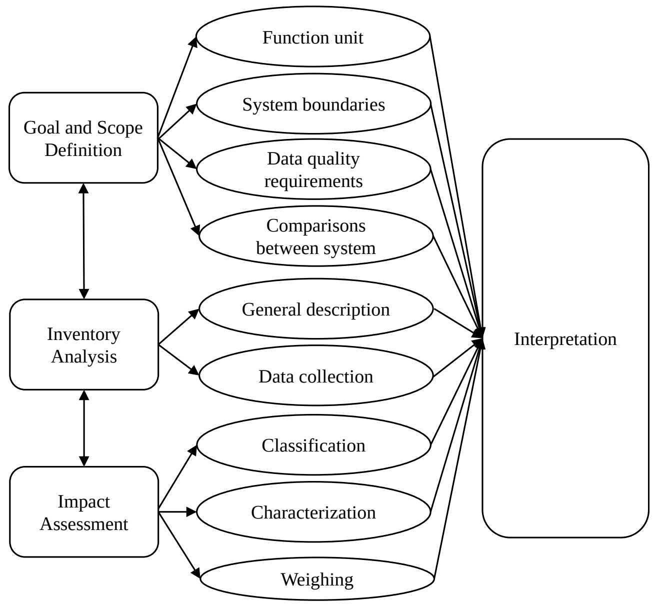

Fig. 2. Life-cycle assessment framework

3.1 Goal and scope definition

This section specifies the functional unit and system boundaries. In this study, the function unit is defined as different column forms having similar loading capacity. As discussed in Section 2, CFST, CFFT and DSTC are all designed to carry a nominal axial load of 5,622 kN.

This study aims to conduct a cradle-to-grave life-cycle assessment, covering all aspects of the life-cycle process from raw materials to the end of construction waste. A typical life-cycle process for constructions starts from producing structural components, including raw material extraction, concrete mix, steel rolling, etc. Transportation of finished products and on-site construction is considered as well. Maintenance over the whole lifespan is associated with durability of the investigated design alternatives. As for the end-of-life stage, construction demolishing and waste disposal are essential components. All considered phases together with their subsections are schematically shown in Fig. 3.

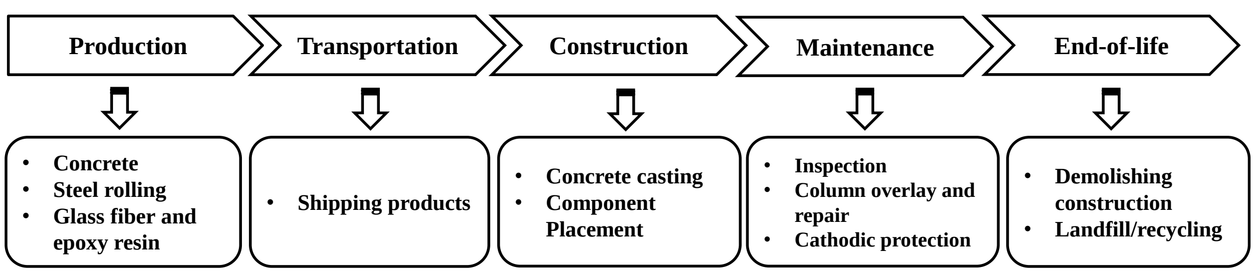

Fig. 3. Flow chart of the studied life-cycle stage

3.2 Maintenance schedule

FRP composites are expected to outperform steel counterparts with respect to enduring behavior which, in turn, differentiates the corresponding maintenance schedules. Herein, previously established deterioration models for CFST, CFFT, and DSTC are incorporated to determine the relevant maintenance schedules. It is assumed that repair actions are taken when the design alternatives are subjected to a certain level of performance loss. According to the time-dependent corrosion model proposed in [81], a CFST column subjected to constant compressive loading and harsh ambient has 10 % performance loss at around year 10.

A series of accelerated experiments were conducted to study the deterioration behavior of GFRP-confined concrete solid columns and GFRP-concrete-steel double-skin tubular columns [82, 83]. The testing regime was designed to represent severe weather exposure for a period of 20 years. Both CFFT and DSTC will end up retaining slightly more than 90 % performance under constant compression loading, i.e., 10 % performance loss at year 20.

To sum up, the assumed baseline maintenance schedule for CFST is every 10 years while the alternatives of CFFT and DSTC will be repaired every 20 years. 10 % original materials will be replaced for every repair action. This is admittedly a simplified maintenance model, which can be easily updated once given more available information associated with deterioration.

3.3 Life-cycle unit processes

As depicted in Fig. 3, the first life-cycle stage is production, covering the whole manufacturing process from raw material ‘in the earth’ to finished products ready for use on site. For concrete, commonly used ingredients include ordinary Portland cement, river gravel, and sand.

Upon completion of the production process, the constituent materials will be transported to the construction site for assembling. All materials are assumed to be transported from local suppliers or those from neighboring cities. Locations were marked on Google map so that mean values of driving distances could be determined accordingly (Table 2).

Table 2 Transportation distance estimation

Phase	Concrete (x_{14})	Steel (x_{15})	FRP (x_{16})
Average distance (km)	34	48	66
Maximum distance (km)	45	110	175
Minimum distance (km)	18	4	4
Number of spots	5	8	4

The following construction phase is associated with activities like mixing, vibrating or pumping concrete and putting shuttering or construction elements in place. Environmental and economic impact at this stage tends to relate to energy consumption and labor intensity. The investigated life-cycle stage, i.e. production, transportation, and construction, that incur at year 0 is also known as the ‘initial stage’.

As discussed in Section 3.2, it is assumed that CFST will be repaired every 10 years while the alternatives will be maintained every 20 years. Common practice in previous studies is to take environmental and economic impacts produced from maintenance actions as a ratio of those from the initial stage [11, 13]. Given a predefined 10 % performance loss at the point where maintenance actions are implemented, the baseline maintenance-to-initial ratio is taken as 0.1, meaning that 10 % material will be replaced or repaired during each individual maintenance action.

During the end-of-life stage, the structural components are expected to be demolished and the resultant construction wastes need to be disposed of in proper ways. Disposal techniques in industry include recycling, landfill, and incineration. Steel is considered as recyclable metallic material that can be refabricated into new products [84]. Herein, the recycled steel weight is taken as 90 % of the original, with the remaining ended up in landfill [13]. Both landfill and recycling apply to concrete wastes. In fact, there has been a growing trend of reusing crushed concrete wastes as aggregates in new concrete [85, 86]. Nevertheless, this seemingly sustainable scenario still has downsides such as quality inconsistency and cost variance [87]. Therefore, concrete wastes are assumed to be shipped to the nearest landfill plant after demolition. In contrast with concrete and steel, neither landfilling nor reuse is the proper solution to FRP treatment. Owing to the potential deleterious substances in composite materials, extra treatment may be required prior to landfill. Incineration, which allows for energy recovery, is thus a more reasonable way for disposal of FRPs [88].

4. Computational process of life-cycle environmental impact and cost

The previous section has elaborated the framework to assess life-cycle environmental impact and cost of the three cases. Given the assessment framework, the following sections present the computational process using established models.

4.1 Environmental impact results

To compute respective environmental impacts of each design alternative, CO_2 emissions associated with individual unit process were collected from the Ecoinvent database [89] or open literatures. The unit CO_2 emissions from producing cement, aggregate, steel tube, steel reinforcement, and GFRP composites are 0.951 kg CO_2/kg, 1.06×10^{-3} kg CO_2/kg [90], 1.802 kg CO_2/kg [91], 1.106 kg CO_2/kg [92], and 2.63 kg CO_2/kg [39], respectively. CO_2 emissions from the construction stage are believed to come from energy consumption of equipment, e.g. generator, truck crane, vibrator, etc., and are associated with use hours. A value of 0.016 kg CO_2 emission for constructing 1 kg concrete is referenced herein [93]. Consider half of the time for steel construction, i.e. 0.008 kg CO_2 emits from constructing per kg steel [94]. As the installation of FRP tube barely requires energy-consumed equipment, the unit CO_2 emission of FRP construction is estimated as 0.004 kg CO_2/kg. Cho and Chae [95] has suggested 0.70×10^{-2} kg CO_2/kg and 0.379×10^{-2} kg CO_2/kg for concrete/steel landfill and steel recycling respectively, while incinerating 1 kg GFRP is associated with 0.61 kg CO_2 emission [96]. The abovementioned GWP factors are listed in Table 3 along with the material consumption of the studied cases.

Given the predefined life-cycle model and inventory data collection, the total CO_2 emissions $Total_{CO_2}$ of investigated design alternative can be calculated as

$$Total_{CO_2}=P_{CO_2}+T_{CO_2}+C_{CO_2}+M_{CO_2}+E_{CO_2} \quad (6)$$

where P_{CO_2}, T_{CO_2}, C_{CO_2}, M_{CO_2}, and E_{CO_2} = CO_2 emission from production, transportation, construction, maintenance, and end-of-life stages, respectively [11, 97].

During the initial stage, CO_2 released from production phase is $P_{CO_2} = \sum_{i=1}^{n} m_i \cdot C_{mi}$, where m_i = the amount of the associated material *i* (kg or *t*), *n* = numbers of material types, and C_{mi} = the unit CO_2 emission associated with unit production process (kg CO_2/kg).

CO_2 emission produced from transportation process is $T_{CO_2} = \sum_{i=1}^{n} m_i \cdot d_i \cdot C_{ti}$, where d_i = transportation distances (km) and C_{ti} = the unit CO_2 emission for transporting 1 kg material (kg CO_2/t·km).

CO_2 released from construction phase is computed as $C_{CO_2} = \sum_{i=1}^{n} m_i \cdot C_{ci}$, where C_{ci} = the unit CO_2 emission factor associated with unit construction process (kg CO_2/kg). Based on previous durability experimental data [81-83], 10 % performance loss is assumed every 10 years for CFST and every 20 years for CFFT and DSTC. Therefore, 10 % of original materials are assumed to be replaced or repaired associated with each maintenance action. CO_2 emitted from each maintenance action during the service stage is thus taken as 10 % of those emitted from the initial stage. Thus, $M_{CO_2} = \left[\left(P_{CO_2}+T_{CO_2}+C_{CO_2}\right)\times 0.1\right] \cdot t_m$, where t_m = times of maintenance actions within the service life. CO_2 emission from the end-of-life phase is $E_{CO_2} = \sum_{i=1}^{n}\left(m_i \cdot C_d - m_{salvage} \cdot C_{salvage}\right)$, where $m_{salvage}$, C_d and $C_{salvage}$ = the amount of treated waste, the unit CO_2 emission for landfilling/incinerating and recycling 1 kg waste, respectively.

The total life-cycle CO_2 emissions of all three investigated cases are compared as illustrated in Table 3 and Fig. 4. CFFT obviously presents the lowest environmental impact, only half the emission of DSTC. DSTC emits about 50 % less CO_2 than CFST does, which is second only to CFFT regarding environmental benefits. Despite 50 % reduction of concrete consumption comparing to CFFT, the presence of inner steel tube significantly increases CO_2 emission from producing DSTC. However, the disadvantage is later offset by less emissions from maintenance stage. For the benchmark scenario CFST, CO_2 emissions from the production and maintenance phases account for similar fractions, around 50 %, of the total. For the other two cases, emissions associated with production hold the largest shares while maintenance emission only account for 30 % of the total. Transportation and end-of-life processes only contribute limited share of emission.

Table 3 Life-cycle environmental impact results

Column	**Life-cycle stage**	**Consumed material**		**Amount**	**Unit**	**GWP coefficient (kg CO_2/kg)**	**GWP result (kg CO_2eq)**
CFST	Production	Concrete	Cement	244	kg	0.951	232.04
			River gravel	732	kg	0.00106	0.78

			Sand	427	kg	0.00106	0.45
		Steel tube		300	kg	1.802	541.29
		Reinforcing steel bars		177	kg	1.106	196.09
		Sum					**970.64**
	Transportation	Concrete		1.52×34	t·km	0.6	31.01
		Steel tube		0.3×48	t·km	0.6	8.64
		Reinforcing steel bars		0.18×48	t·km	0.6	5.10
		Sum					**44.75**
	Construction	Concrete		1521	kg	0.016	24.33
		Steel tube		300	kg	0.008	2.40
		Reinforcing steel bars		177	kg	0.008	1.42
		Sum					**28.15**
	Maintenance	**Sum**					**939.18**
	End-of-life	Concrete (landfill)		1521	kg	0.007	10.64
		Steel tube (landfill)		30	kg	0.007	0.21
		Steel tube (recycling)		270	kg	0.00379	1.02
		Reinforcement (landfill)		18	kg	0.007	0.12
		Reinforcement (recycling)		160	kg	0.00379	0.60
		Sum					**12.61**
	Sum						**1995.33**
CFFT	Production	Concrete	Cement	122	kg	0.951	117.17
			River gravel	215	kg	0.00106	
			Sand	418	kg	0.00106	
			water	61	kg	0.00091	0.06
		FRP tube		31	kg	9.35	293.74
		Sum					**410.96**
	Transportation	Concrete		0.85×34	t·km	0.6	17.34
		FRP		0.0314×66	t·km	0.6	1.24
		Sum					**18.58**
	Construction	Concrete		855	kg	0.016	13.68
		FRP tube		31	kg	0.004	0.13
		Sum					**13.81**
	Maintenance	**Sum**					**177.34**
	End-of-life	Concrete (landfill)		855	kg	0.007	5.99
		FRP tube (incineration)		31	kg	0.61	19.16
		Sum					**25.15**
	Sum						**645.85**
DSTC	Production	Concrete	Cement	63	kg	0.951	60.26
			River gravel	111	kg	0.00106	
			Sand	215	kg	0.00106	

	Water	32	kg	0.00091	0.03
	Steel tube	268	kg	1.802	483.50
	FRP tube	30	kg	9.35	284.69
	Sum				**828.48**
Transportation	Concrete	0.419×34	t·km	0.6	8.55
	Steel tube	0.268×48	kg	0.6	7.72
	FRP tube	0.03×66	t·km	0.6	1.20
	Sum				**17.47**
Construction	Concrete	419	kg	0.016	6.71
	Steel tube	268	kg	0.008	2.15
	FRP tube	30	kg	0.004	0.12
	Sum				**8.97**
Maintenance	**Sum**				**341.97**
End-of-life	Concrete (landfill)	419	kg	0.007	2.93
	Steel tube (recycling)	241	kg	0.00379	0.92
	Steel tube (landfill)	27		0.007	0.19
	FRP tube (incineration)	30	kg	0.61	18.57
	Sum				**22.61**
Sum					**1219.50**

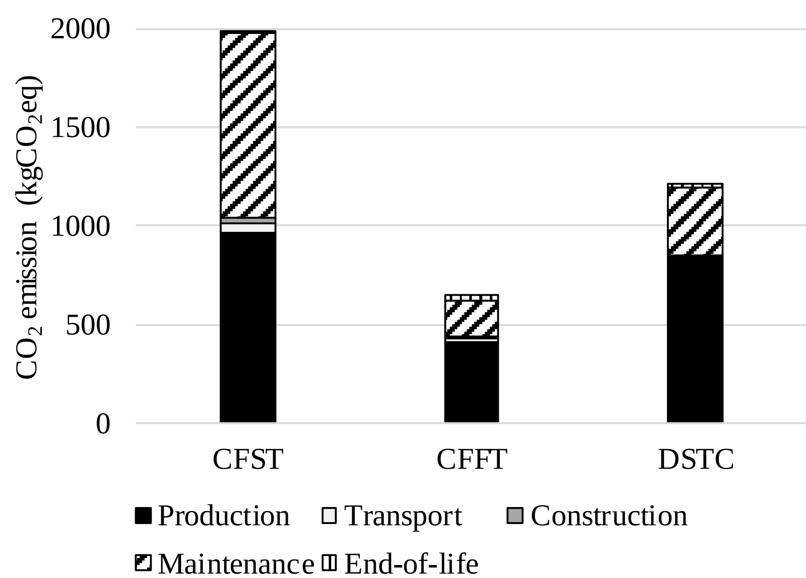

Fig. 4. Comparison of CO_2 emission for three design alternatives

Sensitivity analysis is conducted by varying the baseline maintenance-to-initial ratio from 0 to 0.4. Compared to CFFT and DSTC, the effect seems more prominent on CFST. The life-cycle environmental impact increases significantly as the ratio increases as shown in Fig. 5. However, CFFT remains the most environmentally-friendly alternative while CFST is the least in any case.

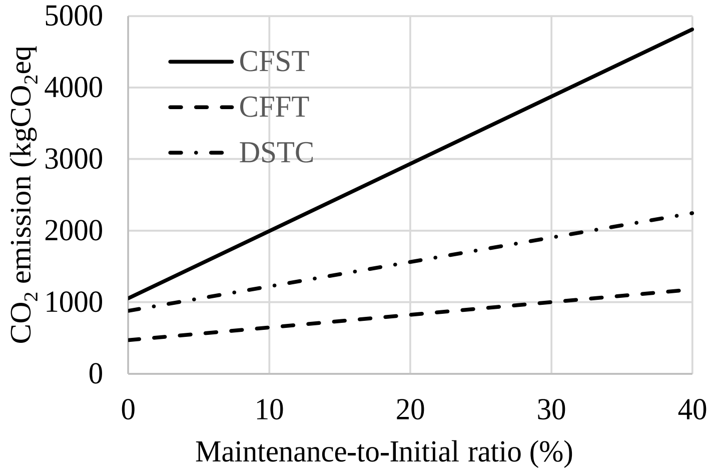

Fig. 5. Life-cycle environmental impact under different maintenance-to-initial ratios

4.2 Life-cycle cost results

In this section, initial cost refers to the sum of material/production cost, transportation cost, and construction cost. Individual costs of related materials are displayed in Table 4. Unlike environmental impact that is associated with energy consumption of equipment use, construction cost has more to do with labor use over machinery use with respect to concreting, erection, installation, etc. A labor rate, referred to the unit labor-to-material cost ratio, is introduced to roughly estimate the construction cost. It is well known that labor costs vary from one country to another. Average labor rate of Australia, UK, and US for concrete, steel reinforcement, and structural steel derived from [98] are 2.32, 0.2, and 0.27, respectively. As FRP tubes are reportedly much less labor-intensive and easier for installation [35, 99], the labor rate for GFRP construction is accordingly reduced to 0.1. The same maintenance schedule is applied to life-cycle cost analysis, with each maintenance action costing 10 % of the initial cost. The unit costs related to end-of-life stage are also listed in Table 4, where the costs were converted with present inflation rate via the calculator provided on http://inflationdata.com/Inflation/Inflation_Rate/HistoricalInflation.aspx.

Table 4 Unit cost data of the studied raw materials

Item	Unit price (USD)	Source
Ready mix concrete C35	177 $/m^3	https://tricityreadymix.com/price-list/
Ready mix concrete C40	186 $/m^3	
Carbon steel bars	0.63 $/kg	https://worldsteelprices.com/
Carbon steel sections	0.78 $/kg	
GFRP tube	10.71 $/m^2	Local supplier
Demolition-concrete	124.2 $/m^3	[13]
Landfill rate	0.089 $/kg	[13]
GFRP incineration	0.23 $/kg	[100]
Carbon steel-scrap value	0.11 $/kg	[13]

Given the inventory data in Table 4 and the consumed material amount listed in Table 3, the total life cycle cost can be computed as follows [13]:

$$LCC = \sum_{t=0}^{T} \frac{C_t}{(1+\gamma)^t} \qquad (7)$$

where t = the year of incurred cost, T = the investigated period, C_t = the cost incurred at the corresponding year, and γ = the monetary discount rate.

Incorporating discount rate is to reflect the potential monetary inflation or deflation over the service life. Herein, the discount rate is taken as 3.3 % [101]. The life-cycle cost $C_t = C_P + C_C + C_M + C_E$, where C_P, C_C, C_M, and C_E refer to production, construction, maintenance, and end-of-life cost, respectively. The discount rate is not applied to the initial stage, i.e., production and construction, as these activities all incur at year 0. Therefore, $C_P + C_C = \sum_{i=1}^{n} m_{m,i} \cdot c_{m,i} + w_i \cdot \sum_{i=1}^{n} m_{m,i} \cdot c_{m,i}$, where $c_{m,i}$ = unit price of manufacturing material i (USD/kg or USD/m^3) and $w_{m,i}$ = the predefined labor ratio. Considering the monetary fluctuation over the studied period, $C_M = \sum_{t=1}^{T} (C_P + C_C) \cdot w$ and $C_E = m_{E,i} \cdot c_{E,i} - m_{s,i} \cdot c_{E,i}$, where w = the assumed percentages of maintenance cost to the corresponding production and construction costs, $m_{E,i}$ = amount of material to be disposed (kg or m^3), $c_{E,i}$ = cost of demolishing, incinerating, landfilling or recycling a unit amount of material i (USD/kg or USD/m^3), and $m_{s,i}$ = amount of material to be recycled (kg).

Given the presumably defined life-cycle model and unit cost inventory, life-cycle costs for three design alternatives were accordingly calculated using Eq. (7). The aggregated production and construction cost is denoted as the initial cost incurred at year 0. Fig. 6 presents the life-cycle cost breakdown for the initial, maintenance, and end-of-life stages. CFST apparently has the cheapest initial cost with CFFT second to it. The initial cost of CFFT and DSTC are nearly 14 % and 30 % more than that of CFST, respectively, mainly attributed to higher material price of FRP composites and structural steel. That said, the drawback of FRP initial cost is offset at later stage, i.e., service duration, by lower maintenance cost. CFFT and DSTC have around 50 % maintenance cost reduction compared to their CFST counterpart. Due to the higher salvaged value of steel, DSTC has the lowest end-of-life cost among three. In balance, CFFT almost costs the same as does CFST despite the higher initial cost.

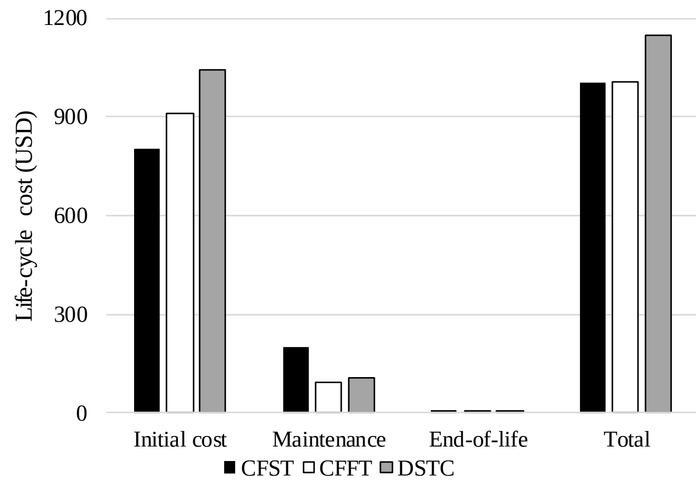

Fig. 6. Comparison of life-cycle costs at different stages

The life-cycle cost results are also presented in a way such that the costs are added up to the total value (Fig. 7). Given the baseline discount rate of 3.3 %, CFST starts with initial cost advantage but ends up with a similar life-cycle cost with CFFT due to more intensive maintenance actions throughout the studied time period.

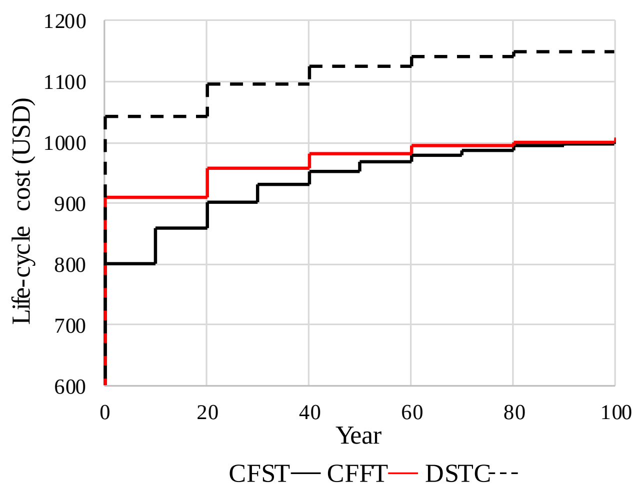

Fig. 7. Comparison of life-cycle costs over time given $\gamma = 3.3\%$

The results of local sensitivity analysis are presented in Figs. 8 and 9. Fig. 8 reveals that discount rate has significant effect on the resultant life-cycle costs. CFST is the costliest alternative given discount rates less than 1 %. Given discount rates between 1 % and 3.3 %, life-cycle cost of CFST remains intermediate between CFFT and DSTC. As discount rate increases, life-cycle costs of CFST and CFFT come closer with DSTC costing the most.

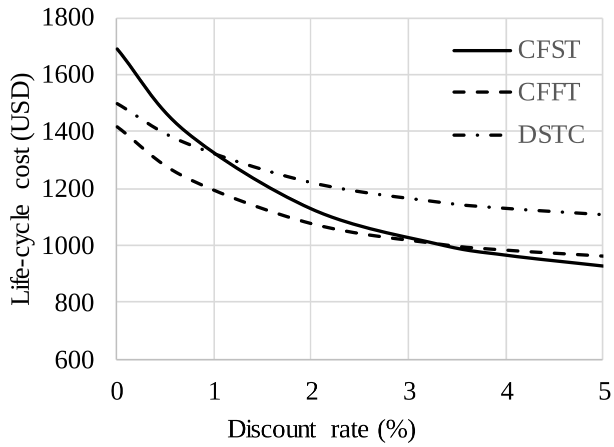

Fig. 8. Life-cycle cost given varied discount rates

As illustrated in Fig. 9, life-cycle cost increases as maintenance-to-initial ratio increases. DSTC is the costliest alternative given a maintenance-to-initial ratio of less than 25 %. Given a ratio between 10 % and 25 %, the life-cycle cost of CFST remains intermediate between CFFT and DSTC. DSTC remains comparatively expensive than CFFT irrespective of the maintenance-to-initial ratio. As the ratio increases, the life-cycle cost of CFST becomes the most expensive alternative of all.

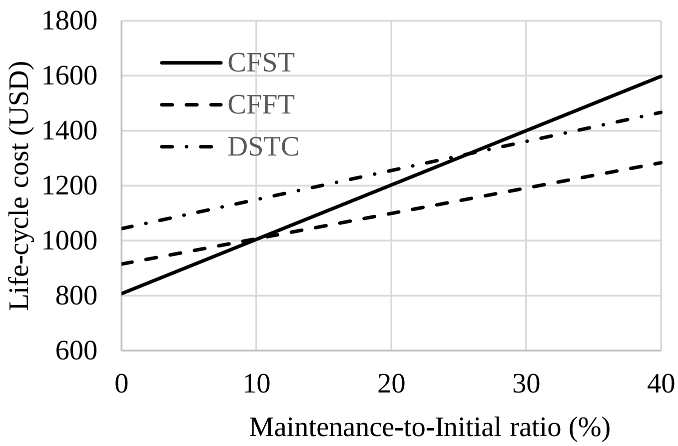

Fig. 9. Life-cycle cost under different maintenance-to-initial ratios

Taken together the deterministic life-cycle results, FRP-confined scenarios display prominent environmental merits in the long run. DSTC, though costs more than CFST over the studied period, remains a potentially advantageous alternative when more practical conditions, e.g. flexural resistance, seismic performance, fire resistance, etc., are considered [20].

5. Probabilistic assessment and sensitivity analysis considering uncertainties

5.1 Sensitivity analysis techniques

The above deterministic results have shed some lights on life-cycle environmental impact and cost assessment of the investigated three design alternatives. It is worth noting that the deterministic results were derived from historical datasets and reasonable presumptions without considering the uncertainties during life-cycle modeling process.

To embody the effect of uncertainty propagation, influential factors are identified and given respective distributions, thereby obtaining probabilistic life-cycle results. This process is implemented via Monte Carlo Simulation (MCS) which entails N times random sampling.

A subsequent global sensitivity analysis is conducted to determine how input parameters would simultaneously affect the outcome. Sobol's method is introduced to compute both the first order effects and total effects, the results are presented to reveal the sensitivity levels of each individual input parameter.

The fundamental of Sobol's method is briefly introduced as below. The Sobol's total effect index (STE) measures how much input parameter i affects the output, with all potential interactions with other parameters l, m, k... taken into account:

$$S_{\mathrm{i}}^{\mathrm{STE}}=S_{\mathrm{i}}+S_{\mathrm{il}}+S_{\mathrm{im}}+\ldots+S_{\mathrm{ilm}}+\ldots+S_{\mathrm{ilm}\ldots\mathrm{k}} \quad (8)$$

Given an output function $y = f(x)$ entailing n input parameters, an input parameter space $\mathbf{\Omega}^n = (x_i|\ i = 1, 2, \ldots, n)$ is created. With a constant $f_0 = \int_{\Omega^n} f(x)dx \approx \frac{1}{N}\sum_{n=1}^{N} f(x_n)$, the total output variance S is determined by

$$\mathrm{S}=\int_{\Omega^{\mathrm{n}}} f^2\,(x)\text{-}f_0^2 \approx \frac{1}{N}\sum_{n=1}^{N} f^2\,(x_n)\text{-}f_0^2\, S \quad (9)$$

The first-order Sobol's index S_i is computed as

$$S_i = S\text{-}\frac{1}{2}\left[f(x)\text{-}f\left(x_i, x'_{\text{-}i}\right)\right]^2 \mathrm{d}x\, \mathrm{d}x'_{\text{-}i} \approx S\text{-}\ \frac{1}{2N}\sum_{n=1}^{N}\left[f(x_n)\text{-}f\left(x_{in}\text{-}x'_{\text{-}in}\right)\right]^2 \quad (10)$$

The total Sobol's index S_i^{STE} is computed as [55, 102]

$$S_i^{STE} = \frac{1}{2}\int\left[f(x)\text{-}f\left(x'_i,x_i\right)\right]^2 \mathrm{d}x\mathrm{d}x'_{\text{-i}} \approx \frac{1}{2N}\sum_{n=1}^{N}\left[f(x_n\text{-}f\left(x'_{in}, x_{\text{-}in}\right)\right]^2 \quad (11)$$

where N is MCS sampling size and x_{-i} is the vector complementary to x_i. A flowchart that describes the uncertainty quantification and global sensitivity analysis procedure is depicted in Fig. 10.

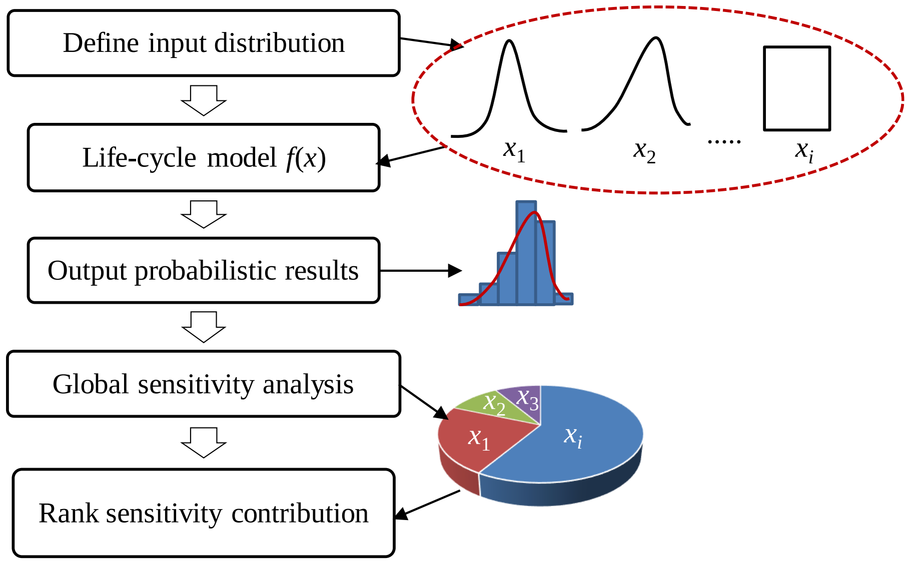

Fig. 10. Flowchart of uncertainty and global sensitivity analysis [102]

5.2 Life-cycle environmental impact considering uncertainties

Referring to [42] and [103], the sensitive parameters include key inputs, e.g., GWP coefficients and maintenance schedule, which are characterized as uniform and normal distributions, respectively. Tables 2, 5, and 7list the random distributions of the selected sensitive parameters, where each of the parameter is designated a number. Given the probability density function of each input parameter, Monte Carlo simulation, the most common technique for uncertainty quantification, is adopted to assess the life-cycle environmental impact. Accordingly, the relevant results are expressed in terms of a probability density function, from which the expected value and the variances can be computed.

Table 5 GWP coefficient of individual item at each life-cycle stage

Phase	Parameter	Assumed value	Distribution (±)	Source
Production	Cement (x_1)	0.951 kg CO_2/kg	40 %	[90]
	River gravel (x_2)	1.06×10^{-3} kg CO_2/kg	20 %	
	Sand (x_2)	1.06×10^{-3} kg CO_2/kg	20 %	
	Steel tube (x_3)	1.802 kg CO_2/kg	20 %	[91]
	Reinforcing bars (x_4)	1.106 kg CO_2/kg	20 %	[92]
	GFRP composites (x_5)	9.35 kg CO_2/kg	40 %	[39]
Transportation	CO_2 emissions from 1 t·km of transportation (x_6)	0.6 kg CO_2/ t·km	20 %	[103]
Construction	Concrete (x_7)	0.016 kg CO_2/kg	40 %	-
	Steel (x_8)	0.008 kg CO_2/kg	20 %	-
	FRP (x_9)	0.004 kg CO_2/kg	40 %	-
End-of-life	Concrete landfill (x_{10})	0.70×10^{-2} kg CO_2/kg	40 %	[95]
	Steel – Recycling (x_{11})	0.379×10^{-2} kg CO_2/kg	20 %	
	Steel – Landfill (x_{12})	0.70×10^{-2} kg CO_2/kg	20 %	
	GFRP incineration (x_{13})	0.61 kg CO_2/kg	40 %	[96]

Based on the MCS results, the maximum, 75% quartile, mean, 25% quartile, and minimum life-cycle CO_2 equivalent emissions are extracted and depicted in Fig. 11. The total CO_2 emission of CFST have the least variation which is around ±25 % while the variations of CFFT and DSTC are both around ±60 %. For the investigated three cases, the uncertainties embedded in the maintenance schedule are shown to contribute the most to the output variance.

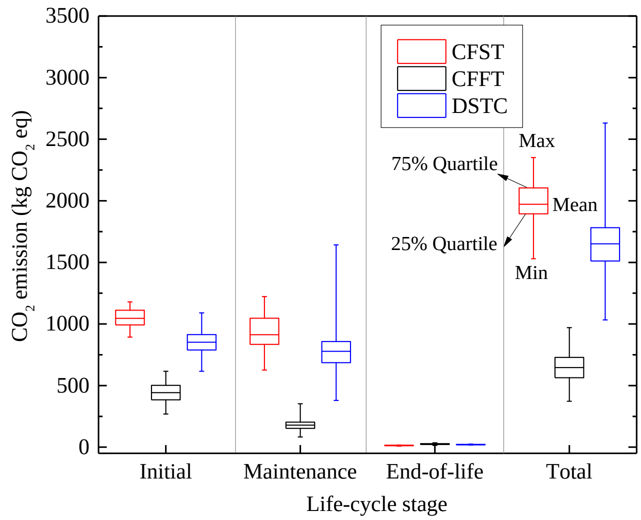

Fig. 11. Life-cycle CO_2 emission results considering uncertainty

Fig. 12a shows the probability density function (PDF) of life-cycle CO_2 emissions associated with the investigated design alternatives. CFFT obviously releases the least CO_2 in any case while an overlap can be seen between CFST and DSTC. Fig. 12b quantifies the possibility that DSTC is more environmental-friendly than CFST, where CI_{GWP} defines the relationship between two impact results of CFST and CFFT, i.e., $CI_{GWP} = Z_{CFST}/Z_{CFFT}$. As shown in Fig. 12b, the possibility that CFST releases more CO_2 than does DSTC is 0.8.

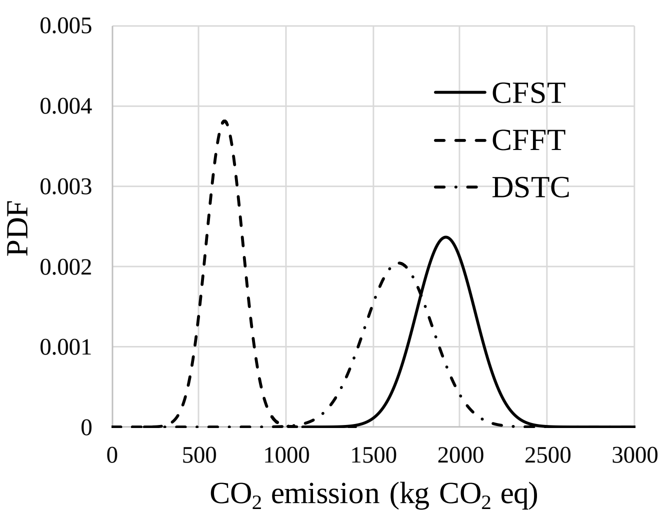

Fig. 12a. PDF of life-cycle CO_2 emission

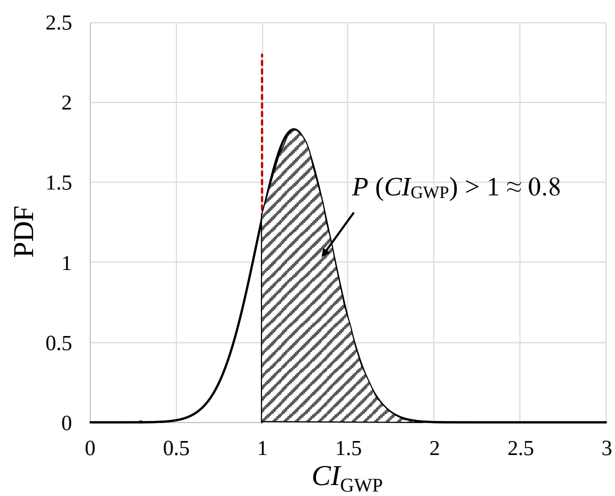

Fig. 12b. PDF of life-cycle CO_2 emission comparison

The Sobol's sensitivity results are listed in Table 6. It is found that for CFST and CFFT, maintenance timing (x_{19}) is the most sensitive parameter. As for DSTC, GWP coefficient of steel tube (x_3) and maintenance timing (x_{19}) are the two most sensitive parameters.

Table 6 Sensitivity analysis results of life-cycle environmental impact using Sobol's method

Parameters \ Sobol's indices	CFST		CFFT		DSTC	
	First-order	Total	First-order	Total	First-order	Total
x_1	0.1062	0.1045	0.3219	0.3209	0.0344	0.0327
x_2	0.0056	0	0.0027	0	0.0021	0
x_3	0.1159	0.1128	-	-	0.4229	0.4214
x_4	0.0477	0.0432	-	-	-	-
x_5	-	-	0.0447	0.0434	0.1459	0.1436
x_6	0.0056	0	0.0026	0	0.0021	0
x_7	0.0056	0	0.0026	0	0.0021	0
x_8	0.0056	0	-	-	0.0021	0
x_9	-	-	0.0026	0	0.0021	0
x_{10}	0.0056	0	0.0026	0	0.0021	0
x_{11}	0.0056	0	-	-	0.0021	0
x_{12}	0.0056	0	-	-	0.0021	0
x_{13}	-	-	0.0026	0	0.0021	0
x_{14}	0.0066	0.0010	0.0067	0.0038	0.0064	0.0043
x_{15}	0.0073	0.0015	-	-	0.0042	0.0023
x_{16}	-	-	0.0029	0.0002	0.0022	0.00008
x_{19}	0.7380	0.7377	0.6318	0.6316	0.3947	0.3956

5.3 Life-cycle cost considering uncertainties

With respect to life-cycle cost, the sensitive parameters are selected as initial cost, discount rate, and maintenance timing (Table 7). Initial cost refers to the sum of production and construction cost, which covers almost all uncertainties of input parameters. The FHWA has suggested an acceptable range for discount rate within 3-5 % while a typical one hovers at 4 % [104]. Herein, a triangular distribution is assumed and the minimum, most likely, and maximum values are 0 %, 3.3 %, and 5 % respectively [101].

Table 7 Random variables for life-cycle cost analysis

Random variable		Distribution	Description
Initial cost (x_{17})		Uniform	± 20 %
Discount rate (x_{18})		Triangular	Min = 0, most likely = 0.33 %, max = 5 %
Maintenance timing (x_{19})	CFST	Normal [42]	Mean = 10 years, COV = 0.15
	CFFT		Mean = 20 years, COV = 0.07
	DSTC		Mean = 20 years, COV = 0.11

The life-cycle cost variation of CFST is around ±40 %, which is slightly larger than those of CFFT and DSTC, i.e., around 30 % (Fig. 13). A clear trend is that the end-of-life cost variations

(±90 %) are larger than maintenance cost variations (around ±60 %) which are larger than initial cost variations (±20 - ±30 %). Therefore, the output variance of life-cycle cost is supposedly attributed to the varying discount rate as its impact is cumulated with time (Equation 7).

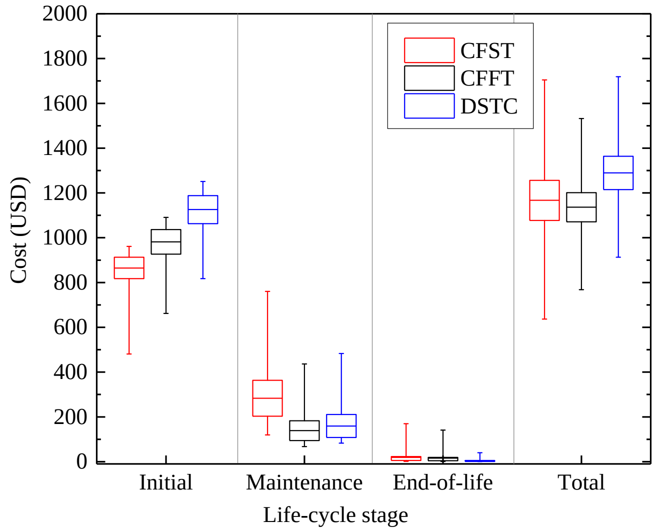

Fig. 13. Life-cycle cost results considering uncertainty

As presented in Fig. 14a, PDFs of life-cycle cost show considerable overlaps between life-cycle cost results of the three cases. PDFs of comparison between the three cases indicate that the probabilities that CFST costs more than does CFFT, CFST costs more than does DSTC, and CFFT costs more than does DSTC are 0.59, 0.25, and 0.14, respectively (Fig. 14b).

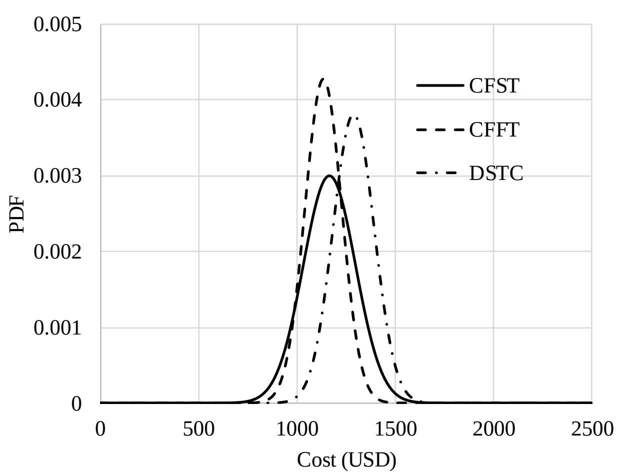

Fig. 14a. PDF of life-cycle cost

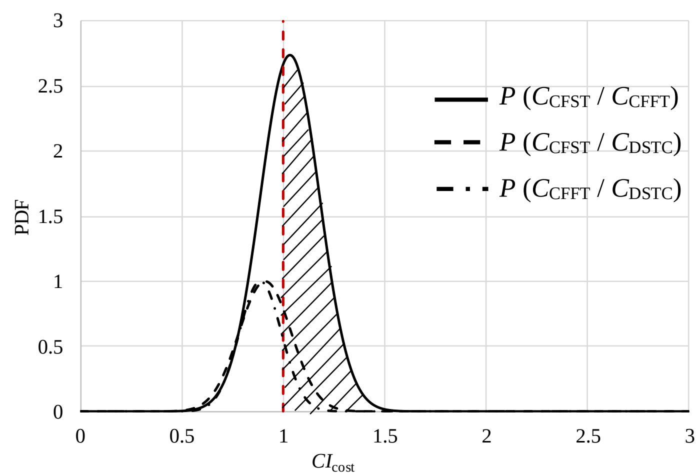

Fig. 14b. PDF of life-cycle cost comparison

The Sobol's sensitivity analysis results are presented in Table 8. It is found that maintenance timing is the most sensitive factor while discount rate is the least. Table 8 also shows that discount rate has no interaction with other parameters.

Table 8 Sensitivity analysis results of life-cycle cost using Sobol's method

Sobol's indices / Parameters	CFST		CFFT		DSTC	
	First-order	Total	First-order	Total	First-order	Total
x_{17}	0.1789	0.1765	0.4843	0.4764	0.4747	0.4747
x_{18}	0.0046	0	0.0086	0	0.0007	0
x_{19}	0.8234	0.8211	0.5236	0.5157	0.5253	0.5253

6. Discussions: further applications

The developed framework of the present study may be extended to other case scenarios such as beams or beam-columns subjected to static and dynamic conditions. This This section focuses on the potential application of the proposed method within other configurations and boundary conditions.

6.1 Beams

Fig. 15 illustrates typical forms of CFFT and DST beams (DSTB) studied in previous research. Test results indicate that DSTB with an inner steel tube eccentrically placed within the outer FRP tube outperforms the alternatives regarding flexural resistance and ductility [105, 106]. However, slip between the infill concrete and steel tubes were spotted in [105, 107, 108]. Attempts were made to address such bonding issues by adding steel rings [107] or shear connectors [106] which, though effective, largely increase steel consumption and labour intensity.

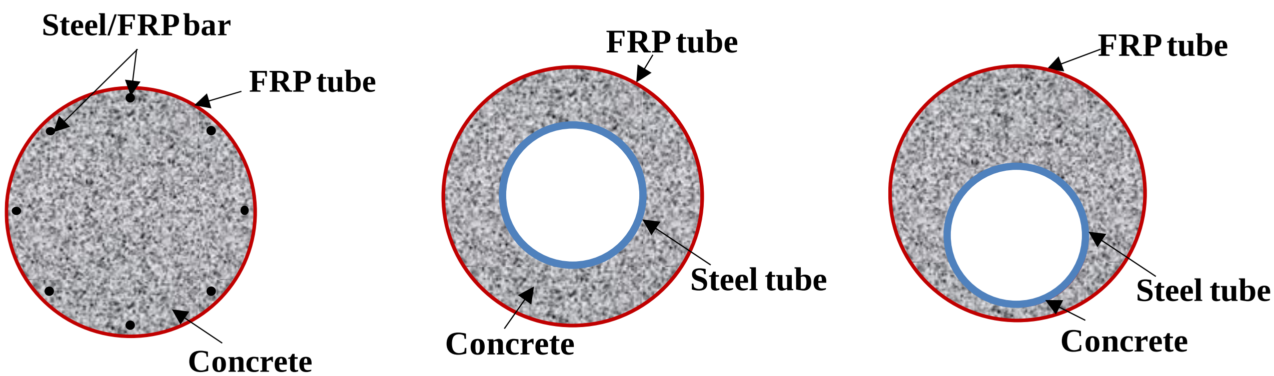

a. CFFT beam [105] b. DSTB (concentric) [105, 107, 108] c. DSTB (eccentric) [105, 106]

Fig. 15. Typical CFFT and DSTB

Therefore, future studies may consider full-scale beams with similar shear resistance, flexural resistance, crack limit, ductility, etc.[109], as comparable case studies for life-cycle environmental impact and cost analysis.

6.2 Seismic performance

Test data regarding CFFT and DST columns, beams, and beam-columns subject to cyclic loading can be found in [22, 28, 110-112]. The seismic performance of CFST and CFFT beam-columns were compared in [112], where CFST showed better ductility and energy dissipation than CFFT. However, the brittleness of CFFT was shown to be compensated by the presence of an inner steel tube [22, 28, 110, 111]. More uncertainties may be considered when analyzing seismic performance.

To associate life-cycle seismic performance with life-cycle environmental impact and cost analysis, earthquake scenarios that a structural element may be experienced during its lifetime need to be assumed [113]. The probabilistic seismic loss should be quantified considering all potential earthquake scenarios which, in turn, can be linked to economic and environmental impact [114].

7. Conclusions

A life-cycle assessment and life-cycle cost analysis (LCA-LCCA) was conducted in this study. The LCA-LCCA aims to evaluate life-cycle performance of comparative concrete-filled steel tubular column (CFST), concrete-filled FRP tubular column (CFFT), and hybrid FRP-concrete-steel double-skin tubular column (DSTC) from environmental and economic perspectives. Apart from deterministic results, uncertainty quantification and global sensitivity analysis results are also presented. First order effects and total effects were computed and parameters were ranked according to their contribution to the output variance of the life-cycle environmental impact and life-cycle cost. The following conclusions can be drawn:

- As can be seen from the deterministic life-cycle environmental results, CFFT is the most environmental-friendly alternative of all with DSTC only second to it. In contrast, life-cycle CO_2 emission of CFST is as much as three times that of CFFT.
- Given a reasonable discount rate of 3.3 %, DSTC has the largest life-cycle cost while CFST and CFFT cost nearly 15 % less than DSTC does. A follow-up local sensitivity analysis demonstrates that the life-cycle cost varies as discount rate varies between 0 and 5 %. CFST is very likely to become the most cost-effective option with increasing discount rate.
- Despite that the deterministic results indicate that CFFT is the most environmentally and economically benefited alternative of all, the probabilistic results tell something different. CFST is potentially more environmental-friendly than DSTC if input uncertainties are considered. The probabilities of each alternative being more cost-effective are presented in the form of probability density functions. Finally, the key influential parameters are identified by means of Sobol's method.
- The above findings are limited to the simplifications and assumptions in some aspects. For instance, very limited information is available in terms of maintenance schedule of the investigated composite structural elements.

- The results are expected to provide more evidence for stakeholders to make decisions by considering the tradeoffs among multiple perspectives associated with novel structural systems. Life-cycle performance of composite structural elements in other case scenarios, e.g., columns, beams or beam-columns subject to static or seismic conditions, will be explored in future work.

Acknowledgments

This study has been supported by National Key R&D Program of China (No. 2019YFB1600702), National Natural Science Foundation of China (Grant No. 51808476), and the Research Grants Council of the Hong Kong Special Administrative Region, China (No.: T22-502/18-R and No. PolyU 15219819). The authors gratefully acknowledge Ms. Yaohan Li for the support in terms of script coding.

References:

[1] Tamiotti L. Trade and climate change: a report by the United Nations Environment Programme and the World Trade Organization: UNEP/Earthprint; 2009.

[2] Miller SA, Horvath A, Monteiro PJM. Readily implementable techniques can cut annual CO_2 emissions from the production of concrete by over 20%. Environmental Research Letters. 2016;11:074029.

[3] Quader MA, Ahmed S, Ghazilla RR, Ahmed S. CO_2 Capture and Storage for the Iron and Steel Manufacturing Industry Challenges and Opportunities. Journal of Applied Science and Agriculture. 2014;9:60-7.

[4] Teng JG, Zhao JL, Yu T, Li LJ, Guo YC. Behavior of FRP-Confined Compound Concrete Containing Recycled Concrete Lumps. Journal of Composites for Construction. 2016;20.

[5] Shi X, Mukhopadhyay A, Zollinger D, Grasley Z. Economic input-output life cycle assessment of concrete pavement containing recycled concrete aggregate. Journal of cleaner production. 2019;225:414-25.

[6] Geng Y, Wang Y, Chen J, Zhao M. Time-dependent behaviour of 100% recycled coarse aggregate concrete filled steel tubes subjected to high sustained load level. Engineering Structures. 2020;210:110353.

[7] Tang Z, Li W, Tam VWY, Yan L. Mechanical performance of CFRP-confined sustainable geopolymeric recycled concrete under axial compression. Engineering Structures. 2020;224:111246

[8] Semendary AA, Svecova D. Factors affecting bond between precast concrete and cast in place ultra high performance concrete (UHPC). Engineering Structures. 2020;216:110746

[9] Wu P, Wu C, Liu Z, Hao H. Investigation of shear performance of UHPC by direct shear tests. Engineering Structures. 2019;183:780-90.

[10] Dai P, Yang L, Wang J, Zhou Y. Compressive strength of concrete-filled stainless steel tube stub columns. Engineering Structures. 2020;205:110106

[11] Dong Y. Performance assessment and design of ultra-high performance concrete (UHPC) structures incorporating life-cycle cost and environmental impacts. Construction and Building Materials. 2018;167:414-25.

[12] Niejenhuis CV, Walbridge S, Hansson C. Life-cycle cost analysis of concrete structures reinforced with stainless steel reinforcing bars. International Association for Bridge and Structural Engineering; 2017. p. 872-9.

[13] Younis A, Ebead U, Judd S. Life cycle cost analysis of structural concrete using seawater, recycled concrete aggregate, and GFRP reinforcement. Construction and Building Materials. 2018;175:152-60.

[14] Han L, Li W, Bjorhovde R. Developments and advanced applications of concrete-filled steel tubular (CFST) structures: Members. Journal of Constructional Steel Research. 2014;100:211-28.

[15] Fardis MN, Khalili H. Concrete encased in fiberglass-reinforced plastic. 1981. p. 440-6.

[16] Yu T, Teng JG. Design of Concrete-Filled FRP Tubular Columns: Provisions in the Chinese Technical Code for Infrastructure Application of FRP Composites. Journal of Composites for Construction. 2011;15:451-61.

[17] Gand AK, Chan T-M, Mottram JT. Civil and structural engineering applications, recent trends, research and developments on pultruded fiber reinforced polymer closed sections: a review. Frontiers of Structural and Civil Engineering. 2013;7:227-44

[18] Mohammed AA, Manalo AC, Ferdous W, Zhuge Y, Vijay PV, Alkinani AQ et al. State-of-the-art of prefabricated FRP composite jackets for structural repair. Engineering Science and Technology, an International Journal. 2020.

[19] Xiao J, Qiang C, Nanni A, Zhang K. Use of sea-sand and seawater in concrete construction: Current status and future opportunities. Construction and Building Materials. 2017;155:1101-11.

[20] Teng JG, Yu T, Wong YL, Dong SL. Hybrid FRP–concrete–steel tubular columns: Concept and behavior. Construction and Building Materials. 2007;21:846-54.

[21] Zhang B, Teng JG, Yu T. Compressive Behavior of Double-Skin Tubular Columns with High-Strength Concrete and a Filament-Wound FRP Tube. Journal of Composites for Construction. 2017;21.

[22] Zhang B, Teng JG, Yu T. Experimental behavior of hybrid FRP–concrete–steel double-skin tubular columns under combined axial compression and cyclic lateral loading. Engineering Structures. 2015;99:214-31.

[23] Wang W, Wu C, Liu Z. Compressive behavior of hybrid double-skin tubular columns with ultra-high performance fiber-reinforced concrete (UHPFRC). Engineering Structures. 2019;180:419-41.

[24] Yang T, Wang W, Liu Z, Wu C, Xu S, Yang Y. Behavior of CFRP-UHPFRC-steel double skin tubular columns against low-velocity impact. Composite Structures. 2020:113284.

[25] Wang W, Wu C, Liu Z, An K, Zeng J-J. Experimental Investigation of the Hybrid FRP-UHPC-Steel Double-Skin Tubular Columns under Lateral Impact Loading. Journal of Composites for Construction. 2020;24:04020041.

[26] Zhao X-L, Han L-H, Lu H. Concrete-filled tubular members and connections: CRC Press; 2010.

[27] Yu T, Zhang B, Cao YB, Teng JG. Behavior of hybrid FRP-concrete-steel double-skin tubular columns subjected to cyclic axial compression. Thin-Walled Structures. 2012;61:196-203.

[28] Zhang B, Yu T, Teng JG. Behavior of concrete-filled FRP tubes under cyclic axial compression. Journal of Composites for Construction. 2015;19:04014060

[29] Wei X, Wen Z, Xiao L, Wu C. Review of fatigue assessment approaches for tubular joints in CFST trusses. International Journal of Fatigue. 2018;113:43-53.

[30] Tian HW, Zhou Z, Wei Y, Lu JP. Behavior and Modeling of Ultra-High Performance Concrete-Filled FRP Tubes Under Cyclic Axial Compression. Journal of Composites for Construction. 2020;24.

[31] Li S, Han L-H, Wang F-C, Hou C-C. Seismic behavior of fire-exposed concrete-filled steel tubular (CFST) columns. Engineering Structures. 2020;224:111085.

[32] Rossi B, Lukic I, Iqbal N, Du G, Cregg D, Borg RP et al. Life cycle impacts assessment of steel, composite, concrete and wooden columns. 2011. p. 277-85.

[33] Han L-H. Investigation on life-cycle based theory of concrete-filled steel tubular (CFST) structures. 8th International Conference on Steel and Aluminium Structures (ICSAS 2016). Hong Kong, China2016.

[34] Hou C-C, Han L-H. Life-cycle performance of deteriorated concrete-filled steel tubular (CFST) structures subject to lateral impact. Thin-Walled Structures. 2018;132:362-74.

[35] Hastak M, Halpin DW. Assessment of life-cycle benefit-cost of composites in construction. Journal of Composites for Construction. 2000;4:103-11.

[36] Hastak M, Mirmiran A, Richard D. A Framework for Life-Cycle Cost Assessment of Composites in Construction. Journal of Reinforced Plastics and Composites. 2016;22:1409-30.

[37] Smith JL. Life-cycle cost analysis of reinforced concrete bridges rehabilitated with CFRP: Univesity of Kentucky; 2015.

[38] Nishizaki I, Takeda N, Ishizuka Y, Shimomura T. A case study of life cycle cost based on a real FRP bridge. 2006. p. 13-5.

[39] Li Y, Yu C, Chen S, Sainey B. The Carbon Footprint Calculation of the GFRP Pedestrian Bridge at Tai-Jiang National Park. International Review for Spatial Planning and Sustainable Development. 2013;1:13-28.

[40] Maxineasa SG, Taranu N, Bejan L, Isopescu D, Banu OM. Environmental impact of carbon fibre-reinforced polymer flexural strengthening solutions of reinforced concrete beams. The International Journal of Life Cycle Assessment. 2015;20:1343-58.

[41] Cadenazzi T, Dotelli G, Rossini M, Nolan S, Nanni A. Cost and environmental analyses of reinforcement alternatives for a concrete bridge. Structure and Infrastructure Engineering. 2020;16:787-802.

[42] Eamon CD, Jensen EA, Grace NF, Shi X. Life-Cycle Cost Analysis of Alternative Reinforcement Materials for Bridge Superstructures Considering Cost and Maintenance Uncertainties. Journal of Materials in Civil Engineering. 2012;24:373-80.

[43] Yang DY, Frangopol DM, Teng J-G. Probabilistic life-cycle optimization of durability-enhancing maintenance actions: Application to FRP strengthening planning. Engineering structures. 2019;188:340-9

[44] Micheli L, Alipour A, Laflamme S, Sarkar P. Performance-based design with life-cycle cost assessment for damping systems integrated in wind excited tall buildings. Engineering Structures. 2019;195:438-51

[45] Basbagill J, Flager F, Lepech M, Fischer M. Application of life-cycle assessment to early stage building design for reduced embodied environmental impacts. Building and Environment. 2013;60:81-92.

[46] Yu D, Tan H, Ruan Y. A future bamboo-structure residential building prototype in China: Life cycle assessment of energy use and carbon emission. Energy and Buildings. 2011;43:2638-46.

[47] Gervásio H, Rebelo C, Moura A, Veljkovic M, da Silva LS. Comparative life cycle assessment of tubular wind towers and foundations–Part 2: Life cycle analysis. Engineering structures. 2014;74:292-9

[48] Lee K-M, Cho H-N, Cha C-J. Life-cycle cost-effective optimum design of steel bridges considering environmental stressors. Engineering Structures. 2006;28:1252-65

[49] Keoleian GA, Kendall A, Dettling JE, Smith VM, Chandler RF, Lepech MD et al. Life Cycle Modeling of Concrete Bridge Design: Comparison of Engineered Cementitious Composite Link Slabs and Conventional Steel Expansion Joints. Journal of Infrastructure Systems. 2005;11:51-60.

[50] ISO. ISO 14040: Environmental Management: Life Cycle Assessment; Principles and Framework. Geneva: ISO; 2006.

[51] Russell-Smith SV, Lepech MD. Life cycle assessment of FRP seismic retrofitting. 2009.

[52] Bueno C, Hauschild MZ, Rossignolo JA, Ometto AR, Mendes NC. Sensitivity analysis of the use of Life Cycle Impact Assessment methods: a case study on building materials. Journal of Cleaner Production. 2016;112:2208-20

[53] Ismaeel WSE. Midpoint and endpoint impact categories in Green building rating systems. Journal of Cleaner Production. 2018;182:783-93.

[54] Kendall A, Keoleian GA, Helfand GE. Integrated life-cycle assessment and life-cycle cost analysis model for concrete bridge deck applications. Journal of Infrastructure Systems. 2008;14:214-22.

[55] Groen EA, Bokkers EAM, Heijungs R, de Boer IJM. Methods for global sensitivity analysis in life cycle assessment. The International Journal of Life Cycle Assessment. 2017;22:1125-37.

[56] Frangopol DM, Dong Y, Sabatino S. Bridge life-cycle performance and cost: analysis, prediction, optimisation and decision-making. Structure and Infrastructure Engineering. 2017;13:1239-57.

[57] Tu B, Fang Z, Dong Y, Frangopol DM. Time-variant reliability analysis of widened deteriorating prestressed concrete bridges considering shrinkage and creep. Engineering Structures. 2017;153:1-16.

[58] Guo H, Dong Y, Gu X. Durability assessment of reinforced concrete structures considering global warming: A performance-based engineering and experimental approach. Construction and Building Materials. 2020;233:117251

[59] Wang Z, Jin W, Dong Y, Frangopol DM. Hierarchical life-cycle design of reinforced concrete structures incorporating durability, economic efficiency and green objectives. Engineering Structures. 2018;157:119-31.

[60] Di Lullo G, Gemechu E, Oni AO, Kumar A. Extending sensitivity analysis using regression to effectively disseminate life cycle assessment results. The International Journal of Life Cycle Assessment. 2020;25:222-39.

[61] Igos E, Benetto E, Meyer R, Baustert P, Othoniel B. How to treat uncertainties in life cycle assessment studies? The International Journal of Life Cycle Assessment. 2019;24:794-807 %@ 1614-7502.

[62] Pannier M-L, Schalbart P, Peuportier B. Comprehensive assessment of sensitivity analysis methods for the identification of influential factors in building life cycle assessment. Journal of Cleaner Production. 2018;199:466-80.

[63] Di Lullo G, Oni AO, Gemechu E, Kumar A. Developing a greenhouse gas life cycle assessment framework for natural gas transmission pipelines. Journal of Natural Gas Science and Engineering. 2020;75:103136 %@ 1875-5100.

[64] EN. EN 1993-1-1: Design of steel structures-Part 1-1: General rules and rules for buildings. European Committee for Standardization, Brussels2005.

[65] EN. 1-1. Eurocode 2: Design of concrete structures–Part 1-1: General rules and rules for buildings. European Committee for Standardization (CEN)2004.

[66] Pel L, Jaspers S, Pereira F, Pimienta P, Carré H. Combined NMR moisture, temperature and pressure measurements during heating. EDP Sciences; 2013. p. 03005.

[67] Teng JG, Jiang T, Lam L, Luo YZ. Refinement of a design-oriented stress–strain model for FRP-confined concrete. Journal of Composites for Construction. 2009;13:269-78.

[68] Xiao QG, Teng JG, Yu T. Behavior and modeling of confined high-strength concrete. Journal of Composites for Construction. 2010;14:249-59.

[69] Ozbakkaloglu T, Lim JC, Vincent T. FRP-confined concrete in circular sections: Review and assessment of stress–strain models. Engineering Structures. 2013;49:1068-88.

[70] Lin G, Teng JG. Three-Dimensional Finite-Element Analysis of FRP-Confined Circular Concrete Columns under Eccentric Loading. Journal of Composites for Construction. 2017;21.

[71] Yu T, Teng JG, Wong YL. Stress-strain behavior of concrete in hybrid FRP-concrete-steel double-skin tubular columns. Journal of structural engineering. 2010;136:379-89.

[72] Xie P. Behavior of large-scale hybrid FRP-concrete-steel double-skin tubular columns subjected to concentric and eccentric compression. Hong Kong, China: The Hong Kong Polytechnic University; 2018.

[73] Zhang B. Hybrid FRP-concrete-steel double-skin tubular columns under static and cyclic loading. 2015.

[74] Li YL, Zhao XL, Raman RKS. Mechanical properties of seawater and sea sand concrete-filled FRP tubes in artificial seawater. Construction and Building Materials. 2018;191:977-93.

[75] Zhang B, Teng JG, Yu T. Compressive behavior of double-skin tubular columns with high-strength concrete and a filament-wound FRP tube. Journal of Composites for Construction. 2017;21:04017029.

[76] Yu T, Teng JG, Wong YL, Dong SL. Finite element modeling of confined concrete-I: Drucker–Prager type plasticity model. Engineering Structures. 2010;32:665-79.

[77] Yu T, Teng JG, Wong YL, Dong SL. Finite element modeling of confined concrete-II: Plastic-damage model. Engineering Structures. 2010;32:680-91.

[78] Ozbakkaloglu T, Fanggi BAL, Zheng J. Confinement model for concrete in circular and square FRP–concrete–steel double-skin composite columns. Materials & Design. 2016;96:458-69.

[79] Wang Z, Dong Y, Jin WL. Life-cycle cost analysis of deteriorating civil infrastructures incorporating social sustainability. Journal of Infrastructure Systems. 2020:(in press).

[80] Beatty TL. Life-cycle cost analysis primer: US Department of Transportation: Federal Highway Administration; 2002.

[81] Wang, Cao MM, Sun HJ. Time-dependent reliability analysis of circular CFST stub columns under environmental corrosion. Pacific Science Review. 2014;16:201-6.

[82] Wang S, ElGawady MA. Effects of hybrid water immersion, environmental exposures, and axial load on the mechanical properties of concrete filled epoxy-based glass fiber reinforced polymer tubes. Construction and Building Materials. 2019;194:311-21.

[83] Wang S, ElGawady MA. Durability of Hollow-Core GFRP–Concrete–Steel Columns under Severe Weather Conditions. Journal of Composites for Construction. 2019;23:04018078.

[84] Broadbent C. Steel's recyclability: demonstrating the benefits of recycling steel to achieve a circular economy. The International Journal of Life Cycle Assessment. 2016;21:1658-65.

[85] Aslani F, Ma G, Wan DLY, Muselin G. Development of high-performance self-compacting concrete using waste recycled concrete aggregates and rubber granules. Journal of Cleaner Production. 2018;182:553-66.

[86] Yap SP, Chen PZC, Goh Y, Ibrahim HA, Mo KH, Yuen CW. Characterization of pervious concrete with blended natural aggregate and recycled concrete aggregates. Journal of Cleaner Production. 2018;181:155-65.

[87] Silva RV, De Brito J, Dhir RK. Availability and processing of recycled aggregates within the construction and demolition supply chain: A review. Journal of Cleaner Production. 2017;143:598-614.

[88] Duflou JR, Deng Y, Van Acker K, Dewulf W. Do fiber-reinforced polymer composites provide environmentally benign alternatives? A life-cycle-assessment-based study. MRS Bulletin. 2012;37:374-82.

[89] Hedemann J, König U, Cuche A, Egli N. Technical documentation of the ecoinvent database (Final report ecoinvent data v2). 2007.

[90] Müller HS, Breiner R, Moffatt JS, Haist M. Design and properties of sustainable concrete. Procedia Engineering. 2014;95:290-304.

[91] Markus E. Cradle-to-gate life cycle inventory: Canadian and US steel production by mill type. Athena Soustainable Materials Institute: Ottawa, ON, Canada; 2002. p. 3-12.

[92] Stengel T, Schießl P. Life cycle assessment (LCA) of ultra high performance concrete (UHPC) structures. Eco-efficient Construction and Building Materials2014. p. 528-64.

[93] du béton F. Environmental Design: State-of-the-art report: International Federation for Structural Concrete (fib); 2004.

[94] Dabhade UD, Hedaoo NA, Gupta DLM, Ronghe DGN. Time and cost evaluation of construction of steel framed composite floor with precast concrete floor structure. 2009. p. 139-48.

[95] Cho S-H, Chae C-U. A Study on Life Cycle CO_2 Emissions of Low-Carbon Building in South Korea. Sustainability. 2016;8.

[96] Vo Dong PA, Azzaro-Pantel C, Boix M, Jacquemin L, Domenech S. Modelling of Environmental Impacts and Economic Benefits of Fibre Reinforced Polymers Composite Recycling Pathways. Computer Aided Chemical Engineering. 2015;37:2009-14.

[97] Bouhaya L, Le Roy R, Feraille-Fresnet Ald. Simplified environmental study on innovative bridge structure. Environmental science & technology. 2009;43:2066-71.

[98] Chan T, Aibinu A. A Comparison of Construction Cost and Technology Choice. International Congress on Construction Management Research. Montreal, Canada2012. p. 61.

[99] Zoghi M. The international handbook of FRP composites in civil engineering: CRC Press; 2013.

[100] Halliwell S. End of life options for composite waste recycle, reuse or dispose. National Composites Network Best Practice Guide; 2006.

[101] Ilg P, Hoehne C, Guenther E. High-performance materials in infrastructure: a review of applied life cycle costing and its drivers–the case of fiber-reinforced composites. Journal of Cleaner Production. 2016;112:926-45.

[102] Bilal N. Implementation of Sobol’s method of global sensitivity analysis to a compressor simulation model. 22nd International Compressor Engineering Conference at Purdue2014.

[103] Welsh-Huggins SJ, Liel AB, Cook SM. Reduce, Reuse, Resilient? Life-Cycle Seismic and Environmental Performance of Buildings with Alternative Concretes. Journal of Infrastructure Systems. 2020;26:04019033.

[104] Walls J, Smith MR. Life-cycle cost analysis in pavement design: Interim technical bulletin. United States. Federal Highway Administration; 1998.

[105] Yu T, Wong YL, Teng JG, Dong SL, Lam ES. Flexural behavior of hybrid FRP-concrete-steel double-skin tubular members. Journal of Composites for Construction. 2006;10:443-52.

[106] Zhao JL, Teng JG, Yu T, Li LJ. Behavior of large-scale hybrid FRP–concrete–steel double-skin tubular beams with shear connectors. Journal of Composites for Construction. 2016;20:04016015

[107] Idris Y, Ozbakkaloglu T. Flexural behavior of FRP-HSC-steel composite beams. Thin-Walled Structures. 2014;80:207-16

[108] Liu M, Qian J. Moment-curvature relationship of FRP-concrete-steel double-skin tubular members. Frontiers of architecture and civil engineering in China. 2009;3:25-31.

[109] Dong S, Li C, Xian G. Environmental Impacts of Glass-and Carbon-Fiber-Reinforced Polymer Bar-Reinforced Seawater and Sea Sand Concrete Beams Used in Marine Environments: An LCA Case Study. Polymers. 2021;13:154.

[110] Ozbakkaloglu T, Idris Y. Seismic behavior of FRP-high-strength concrete–steel double-skin tubular columns. Journal of Structural Engineering. 2014;140:04014019.

[111] Idris Y, Ozbakkaloglu T. Seismic behavior of high-strength concrete-filled FRP tube columns. Journal of Composites for Construction. 2013;17:04013013.

[112] Shao Y. Behavior of FRP-concrete beam-columns under cyclic loading: North Carolina State University; 2003.

[113] Zheng Y, Dong Y. Performance-based assessment of bridges with steel-SMA reinforced piers in a life-cycle context by numerical approach. Bulletin of Earthquake Engineering. 2019;17:1667-88

[114] Anwar GA, Dong Y, Li Y. Performance-based decision-making of buildings under seismic hazard considering long-term loss, sustainability, and resilience. Structure and Infrastructure Engineering. 2020:1-17.